

CONTROL SYSTEM DESIGN TECHNIQUES FOR GUIDED MISSILES

Wagih M. M. * , N. R. Matta ** And Wahid Kassem ***

ABSTRACT

The goal of this paper is a quantitative comparison of two *autopilot* designs for the same high-performance advanced guided missiles. One design is obtained using the linear quadratic optimum control technique of state-space design methodology. The other design is based on use of conventional design methods of pole-placement, root locus and frequency response, both designs are initiated with the same set of requirements for the same vehicle. The comparison considers not only robustness of design but also the complexity of implementing the two designs and the analysis required to validate each design.

1. INTRODUCTION

The controller for a homing guided missiles, in general is a closed-loop system called " *autopilot* ", which is a minor loop inside the main guidance loop. The function of any missile autopilot is threefold: 1) maintain stability of the airframe over the performance envelope, 2) provide adequate airframe response for the guidance system, and 3) reduce sensitivity of guidance performance to vehicle parameter variations and disturbances. The degree to which these functions must be performed is determined by design quality of such autopilot.

So, the purpose of this work is to present a two control design methods of two autopilot for the same high performance advanced tactical missile. One design is obtained using the *conventional* control design methods which are first outlined and discussed in section (3), followed by the other design which is based on use of an effective *modern control* method, in section (4). A direct comparison of the performance of auto pilots designed using classical and modern design procedures has been made in section (5).

Finally, the study that was performed includes a linear analysis of both autopilot designs from *classical* and *modern* viewpoints, also it was shown that the analysis of missile dynamics are linearized about some operating condition or "flight regime".

2. SYSTEM MODELING

A linearized dynamic airframe model was developed for stability analysis of both *autopilot* in the state-space approach, that represents the process under controlled by systems of first-order differential equations. Fixed flight conditions (constant velocity, altitude, mass parameters and maneuvers) results in a linear model of the form that has been useful for design and analysis of controlled high-performance advanced tactical missile.

* Ph. D. student, *Air Defence Forces.*
 ** Doctor Eng.
 *** A.Prof. *Chair of Elect. Equip. And Armament Of A/C, Cairo M.T.c*

2.1. Missile Dynamics

Except for difference in *size, weight and speed* a missile is simply a pilotless aircraft. Hence the aerodynamic equations of a missile are the same as those of an aircraft [4]. Consider the motion of a missile about its *pitch* axis, the linear dynamic equations for the *longitudinal* motion of the missile are represented by the following state-space form

$$\begin{aligned}\Delta \dot{u} &= X_u \Delta u + X_\alpha \alpha + g \theta + X_\delta \delta_e \\ \dot{\alpha} &= \frac{Z_u}{V} \Delta u + \frac{Z_\alpha}{V} \alpha + q + \frac{Z_\delta}{V} \delta_e \\ \dot{q} &= M_u \Delta u + M_\alpha \alpha + M_q q + M_\delta \delta_e \\ \dot{\theta} &= q\end{aligned}\quad (1)$$

For simplicity, the following assumptions has been made:

- * The effect of the change of Δu into the equations for angle of attack α and pitch rate q is negligible: Z_u, M_u, X_u are insignificant.
- ** The pitch angle θ is usually not of interest, hence the differential equation $\dot{\theta} = q$ can be omitted.

In this case (1) gives the following pitch dynamics:

$$\begin{aligned}\dot{\alpha} &= \frac{Z_\alpha}{V} \alpha + q + \frac{Z_\delta}{V} \delta \\ \dot{q} &= M_\alpha \alpha + M_q q + M_\delta \delta\end{aligned}\quad (2)$$

Missile guidance laws are generally expressed in terms of the component of acceleration normal to the velocity vector. Thus the output of interest is the "normal" component of acceleration a_N . In planer case (figure 1).

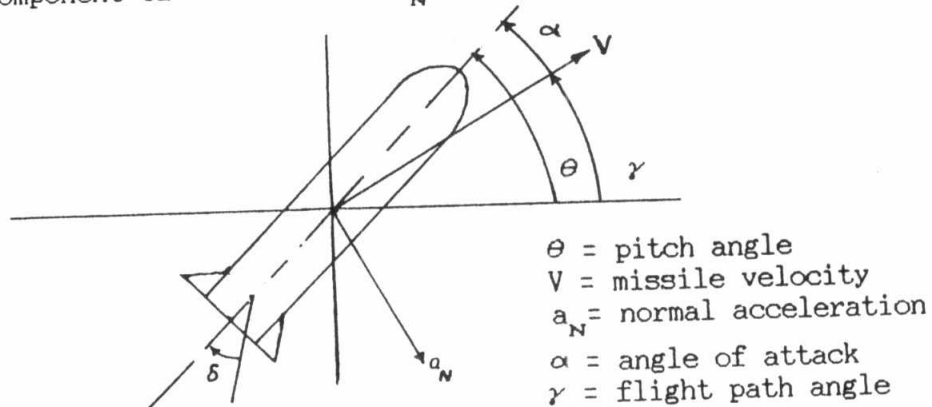


Fig. 1 Missile dynamic variables

$$a_N = -V \dot{\gamma} = -V (q - \dot{\alpha})$$

Using (2).

$$a_N = Z_\alpha \alpha + Z_\delta \delta \quad (3)$$

Equations (2, 3) can be written in the standard state-space form.

$$\begin{aligned}\dot{X} &= A X + B u \\ y &= C X + D u\end{aligned}\quad (4)$$

Where the matrices of the standard representation are:

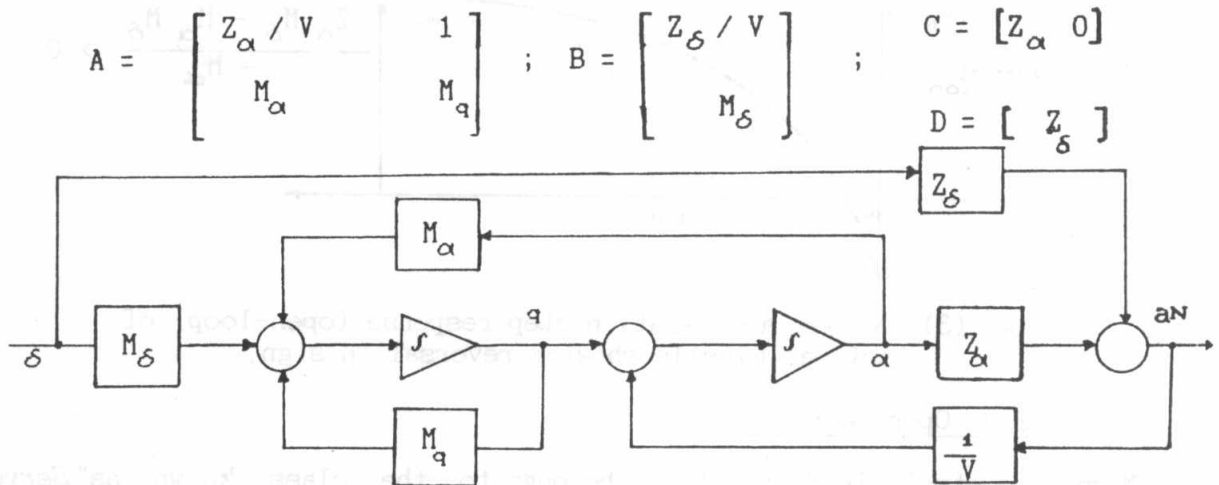


Fig. 2 Block-diagram of missile dynamics showing normal acceleration as output

The transfer function from the input $u=\delta$ to the output $y=a_N$ is given by :

$$H(s) = C (sI - A)^{-1}B + D$$

$$= \frac{Z_\delta (s^2 - M_q s - M_\alpha) + Z_\alpha M_\delta}{s^2 - (M_q + Z_\alpha / V) s + (Z_\alpha / V) M_q - M_\alpha} \quad (5)$$

In a typical missile Z_α , M_α , Z_δ and M_δ are negative. Thus the coefficient of s^2 in the numerator of $H(s)$ is negative. The constant term $(Z_\alpha M_\delta - M_\alpha Z_\delta)$ is (typically) positive. This implies that the numerator of $H(s)$ has a zero in the right half of the s -plane. A transfer function having a right-half plane zero is said to be "nonminimum-phase" and can be the source of considerable difficulty in design of a well-behaved closed-loop control system. We can imagine the problem that might arise by observing that the dc gain $-(Z_\alpha M_\delta - M_\alpha Z_\delta) / M_\alpha$ is (typically) positive but the high-frequency gain Z_δ is (typically) negative. So if a control law is designed to provide negative feedback at dc, unless great care is exercised in the design, it is liable to produce positive feedback at high frequencies. Another peculiarity of the transfer function (5) is that its step response starts out negative and then turns positive, as shown in Figure (3). The initial value of the step response is

$$\lim_{s \rightarrow \infty} s \left[\frac{1}{s} H(s) \right] = Z_\delta < 0$$

and the final value is

$$\lim_{s \rightarrow 0} s \left[\frac{1}{s} H(s) \right] = \frac{Z_\delta Z_\alpha - M_\alpha Z_\delta}{-M_\alpha} > 0$$

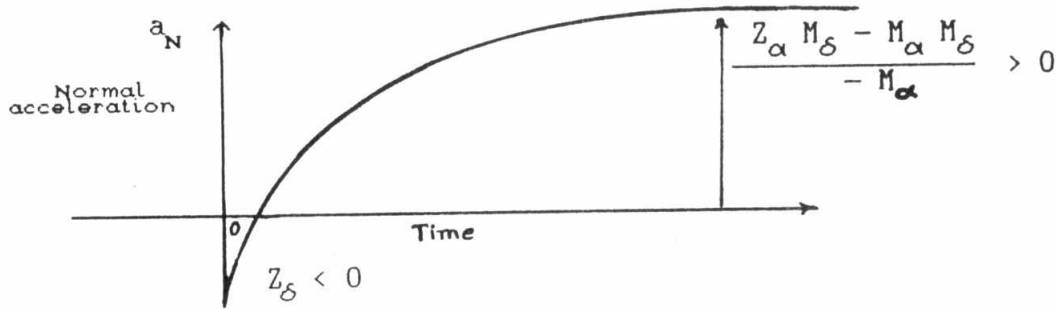


Fig. (3) Normal acceleration step response (open-loop) of tactical missile showing reversal in sign

2.2 Open-Loop Dynamics

Missile control, in distinction, belongs to the class known as "Servo" problems where the desire is to make the normal component of acceleration a_N track a commanded acceleration signal a_{Nc} which is produced by the missile guidance system. Thus it may be necessary to include the dynamics of the actuator which drives the control surface in order to have an adequate model of the process. We use the first-order dynamic model for the actuator that describes the specified response in the form

$$\dot{\delta} = \frac{1}{\tau} (u - \delta) \quad (6)$$

Where u is the input to the actuator and τ is its time constant. In this application, however, we are interested in tracking an acceleration command and hence prefer to use the acceleration error

$$e = a_{Nc} - a_N$$

as a state variable instead of the angle of attack. The derivative of the acceleration error is

$$\dot{e} = \dot{a}_{Nc} - \dot{a}_N$$

We can approach the design problem on the assumption that the commanded acceleration is a constant, and also assume that the aerodynamic coefficients Z_α and Z_δ and the missile speed V are approximately constant. Using all these approximations

$$e = -\dot{a}_N = -Z_\alpha \dot{\alpha} - Z_\delta \dot{\delta}$$

But, from (2)

$$\dot{\alpha} = q + \frac{a_N}{V} = q + \frac{1}{V} (a_{Nc} - e)$$

$$\dot{e} = -Z_\alpha \left[q + \frac{1}{V} (a_{Nc} - e) \right] + \frac{Z_\delta}{\tau} (\delta - u)$$

(7)

The angle of attack α , is

$$\alpha = \frac{1}{Z_\alpha} (a_N - Z_\delta \delta) = \frac{1}{Z_\alpha} (a_{Nc} - e - Z_\delta \delta)$$

Thus the differential equation for the pitch rate, using (2), is

$$\dot{q} = \frac{M_\alpha}{Z_\alpha} (a_{Nc} - e - Z_\delta \delta) + M_q q + M_\delta \delta \quad (8)$$

Both of these equations (6), (7), and (8) are combined to produce an augmented state model.

$$\dot{X} = A X + B u + E a_{Nc} \tag{9}$$

Where the state vector defined by : $X = [e, q, \delta]'$

$$A = \begin{bmatrix} Z_\alpha / V & -Z_\alpha & Z_\delta / \tau \\ -M_\alpha / Z_\alpha & M_q & \tilde{M}_\delta \\ 0 & 0 & -1/\tau \end{bmatrix}; \quad B = \begin{bmatrix} -Z_\delta / \tau \\ 0 \\ 1/\tau \end{bmatrix}; \quad E = \begin{bmatrix} -Z_\alpha / V \\ M_\alpha / Z_\alpha \\ 0 \end{bmatrix}$$

Where $\tilde{M}_\delta = M_\delta - (M_\alpha / Z_\alpha) Z_\delta$

The following numerical data were obtained for a representative highly maneuverable tactical missile [2].

$$V = 1253 \text{ ft/s (mach 1.1)}, \quad Z_\alpha = -4170 \text{ ft/s}^2, \quad Z_\delta = -1115 \text{ ft/s}^2$$

$$M_\alpha = -248 \text{ rad/s}^2, \quad M_\delta = -662 \text{ rad/s}^2, \quad M_q \cong 0, \quad \tau = 0.01$$

Then,

$$A = \begin{bmatrix} -3.328 & 4170. & -111500. \\ -0.0595 & 0. & -595.688 \\ 0. & 0. & -100. \end{bmatrix} \quad B = \begin{bmatrix} 111500. \\ 0. \\ 100. \end{bmatrix} \quad E = \begin{bmatrix} 3.328 \\ 0.0595 \\ 0. \end{bmatrix}$$

The characteristic equation of this system is

$$(s + 1/\tau)(s^2 - (Z_\alpha / V) s - M_\alpha) = 0 \tag{10}$$

Using the numerical data , (10) becomes

$$(s + 100)(s^2 + 3.328 s + 248)$$

With roots at : $s = -100$ (due to actuator)
 and at $s = -1.664 \pm j15.75$ (due to airframe)

The open loop thus has very little damping (0.106) and a natural frequency ω of approximately (15.75 rad/s = 2.51 Hz) would result in a time constant of about 0.4s. The effective way of presenting information about the response of such system is to display in an s-plane diagram the location of the zeros of the characteristic polynomial as in Figure (4). There are, obviously, regions of the s-plane which represent desirable locations for the roots of the system.

3 - CONVENTIONAL CONTROL DESIGN METHOD I

The method to be dealt in this work is the pole-placement method.

3.1 Design Considerations

A shorter closed-loop time constant (high bandwidth) would be desirable for a high performance missile; about 0.2s would be more appropriate. The

bandwidth of a system is governed primarily by its dominant poles, thus we should seek a natural frequency of $\omega \approx 30 \text{ rad/s}$ and $\xi = 0.707$. This suggests a quadratic factor in the closed-loop characteristic polynomial of

$$s^2 + 30\sqrt{2}s + (30)^2 \quad (11)$$

The autopilot design will be done in two steps, First we will design a regulator for a commanded normal acceleration of zero, Second we will compute the feedforward gain to eliminate the steady state error for a nonzero commanded acceleration.

3.2 Regulator Design

We apply the Bass and Gura formula $g = [(QW)']^{-1}(\hat{a} - a)$ to obtain the gains of a controllable, single-input system that will place the poles at any desired location, where Q is the controllability test matrix, W is the triangular matrix defined by (12), \hat{a} is the vector of coefficients for the desired (closed-loop) characteristic polynomial, and a is the vector of coefficients of the open-loop system [1]. From (10) we have the open-loop characteristic equation:

$$s^3 + 103.33 s^2 + 581 s + 24800 = 0$$

The open-loop coefficient vector is

$$a = \begin{bmatrix} 103.33 \\ 581. \\ 24800. \end{bmatrix}; \quad W = \begin{bmatrix} 1 & a_1 & \dots & a_{k-1} \\ 0 & 1 & \dots & a_{k-2} \\ & & \dots & \\ 0 & 0 & & 1 \end{bmatrix} = \begin{bmatrix} 1 & 103.33 & 581. \\ 0 & 1 & 103.33 \\ 0 & 0 & 1. \end{bmatrix} \quad (12)$$

We also find

$$Q = [b, Ab, \dots, A^{k-1}b]$$

$$Q = \begin{bmatrix} 111500. & -11.52 \times 10^6 & 8.77 \times 10^8 \\ 0. & -66.2 \times 10^3 & 6.64 \times 10^6 \\ 100. & 10^4 & 10^6 \end{bmatrix}; \quad QW = \begin{bmatrix} 111500. & 0. & -0.248 \times 10^6 \\ 0. & -66204. & 0.198 \times 10^6 \\ 100. & 333.0 & 24800. \end{bmatrix}$$

$$(QW)^{-1} = \begin{bmatrix} 0.8657 \times 10^{-6} & 0.4544 \times 10^{-4} & 0.9035 \times 10^{-2} \\ 0.1090 \times 10^{-7} & -0.1517 \times 10^{-4} & -0.1215 \times 10^{-4} \\ -0.3637 \times 10^{-8} & 0.2040 \times 10^{-7} & 0.4055 \times 10^{-5} \end{bmatrix}$$

For any choice of closed-loop poles, the feedback gain matrix is given by:

$$g = G' = \begin{bmatrix} g_1 \\ g_2 \\ g_3 \end{bmatrix} = [(QW)']^{-1} \begin{bmatrix} \hat{a}_1 - a_1 \\ \hat{a}_2 - a_2 \\ \hat{a}_3 - a_3 \end{bmatrix} \quad (13)$$

Practical implementation is simplified by omitting the feedback from the control surface deflection. This is achieved by having $g_3 = 0$. From (13), this requirement is satisfied by making :

$$0.9035 \times 10^{-2} (\hat{a}_1 - a_1) - 0.1215 \times 10^{-4} (\hat{a}_2 - a_2) + 0.4055 \times 10^{-5} (\hat{a}_3 - a_3) = 0 \quad (14)$$

But, with a quadratic factor (11), the complete characteristic polynomial is chosen to be

$$(s + \omega_c)(s^2 + 30\sqrt{2}s + 900) = s^3 + \hat{a}_1 s^2 + \hat{a}_2 s + \hat{a}_3$$

Where $\hat{a}_1 = \omega_c + 42.426$; $\hat{a}_2 = 42.426 \omega_c + 900$; $\hat{a}_3 = 900 \omega_c$ (15)

Equations (14) and (15) are solved to yield .

$$\omega_c = 53.8 \quad ; \quad \hat{a}_1 = 96.23 \quad ; \quad \hat{a}_2 = 3182.52 \quad ; \quad \hat{a}_3 = 48420.$$

Then , the roots of the closed loop characteristic polynomial are :

$$s_1 = -53.8 \quad \quad s_{2,3} = -21.2 \pm j21.2$$

The location of the real pole at $s = -\omega_c = 53.8$ is satisfactory , so no feedback gain from the surface deflection is necessary. Thus the gain matrix contains only two nonzero elements :

$$G = [-0.6366 \times 10^{-4} \quad , \quad -0.3929 \times 10^{-1} \quad , \quad 0] \quad (16)$$

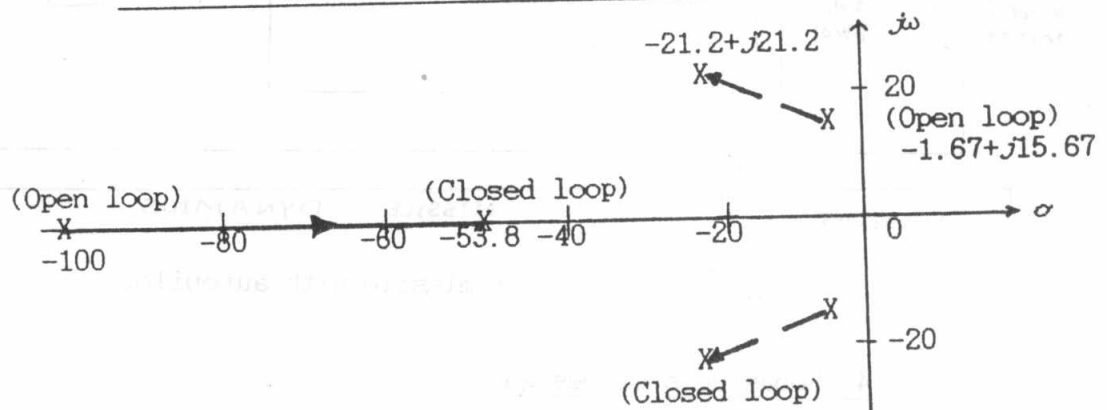


Fig. 4 Open - and closed - loop poles for missile autopilot.

3.3 Feedforward Gain

We have adjusted the gains from the acceleration error ($a_{Nc} - a_N$) and the pitch rate q to provide the desired closed-loop poles, it now remains to set the feedforward gain G_0 to eliminate the steady - state error for a step input of acceleration.

The c matrix for the scalar error is :

$$C = [1 \quad 0 \quad 0]$$

and the closed-loop A_c matrix is

$$A_c = A - BG = \begin{bmatrix} 3.767 & 8550.8 & -111500. \\ -0.0595 & 0. & -595.688 \\ 0.006366 & 3.929 & -100. \end{bmatrix} \quad \text{and} \quad A_c^{-1} = \begin{bmatrix} -0.048 & -8.613 & 105.199 \\ 0.002 & -0.007 & -0.183 \\ 0.000 & -0.001 & -0.0011 \end{bmatrix}$$

Thus $CA_c^{-1} = [-0.048 \quad -8.613 \quad 105.199]$

and $CA_c^{-1}B = 5167.9$

Hence $B^\# = (CA_c^{-1}B)^{-1}CA_c^{-1} = [-9.288 \times 10^{-6} \quad -1.667 \times 10^{-3} \quad 2.02 \times 10^{-2}]$

and , finally , $G_o = B^\#E = -1.2965 \times 10^{-4}$

The autopilot can be implemented as shown in Figure (5). A body-mounted accelerometer measures the actual normal acceleration and a rate gyro measures the actual body pitch rate.

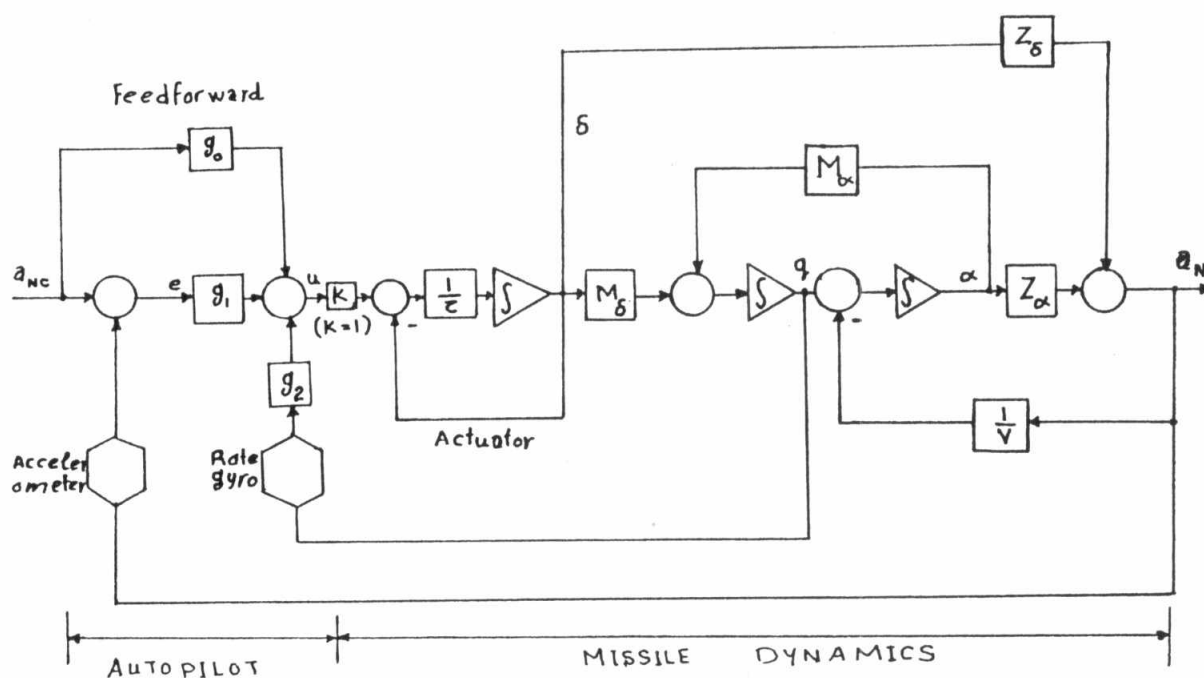


Fig. 5 Dynamics of missile with autopilot

3.4 Robustness Of Design

The "robustness" of the design , i.e., its ability to withstand parameter variations , is of interest. The actuator and airframe dynamics are much more liable to change. Regardless of the true cause of the change , it can be represented by a gain K (with a nominal value of unity) multiplying the control signal u as shown in Figure (5).

The return difference for the loop containing the gain k is :

$$1 + KG (sI - A)^{-1}B$$

The forward loop transmission

$$G_o (s) = G (sI - A)^{-1}B = \frac{-7.09 s^2 + 2601. s + 23606.}{7.09 (-s + 376.) (s + 8.86)} = \frac{N(s)}{D(s)}$$

$$N(s) = 7.09 (-s + 376.) (s + 8.86)$$

The root locus in Figure (6), starts at the nominal of K=1, the loci pass through the poles for which the operation was designed ($s = -15\sqrt{2} \pm j15\sqrt{2}$, and $s = -53.8$) and then continue toward the imaginary axis and ultimately

into the right half-plane. Because of the nonminimum phase zero at $s=376$, the locus has a branch that goes out along the positive real axis as $K \rightarrow \infty$.

The range of gain K for which the system is stable can be found using the Routh or Hurwitz algorithm and is

$$-1.14 < K < 12.21$$

The gain margin is thus 12.2 (or 22 dB) which is more than ample. The frequency at which the root locus crosses the imaginary axis is found to be $\omega = 187$. The right half-plane root-locus plot is shown in Figure (6). It should be noted that the loci, after crossing the imaginary axis, bend over toward the positive real axis and reach it at some positive real value of $s > 376$ the positive zero of $N(s)$. Then one branch goes to the zero and the other goes to $+\infty$.

The Bode plot for the open-loop transmission $G_o(s)$ is shown in Figure (7).

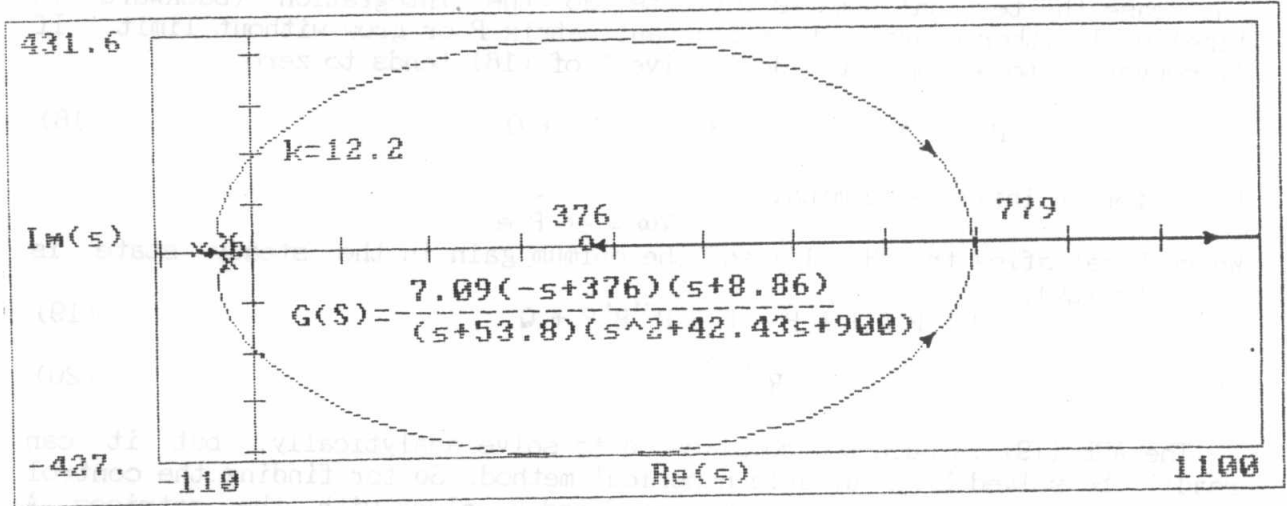


Fig. 6 Root-locus plot for missile autopilot $G(s)$

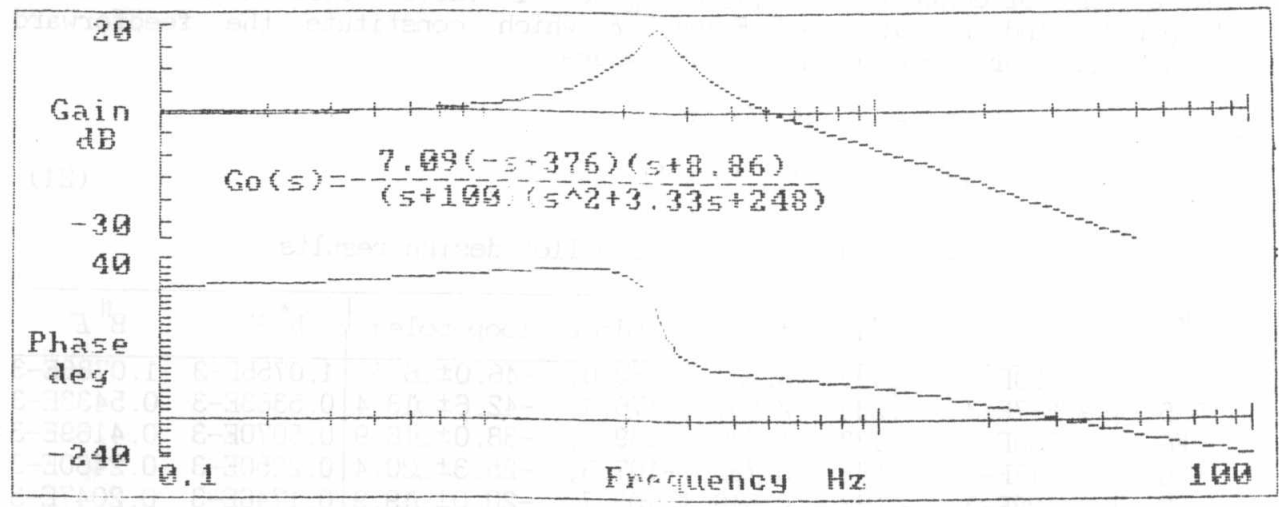


Fig. 7 Bode plot for open-loop transmission for missile autopilot $G_o(s)$

4 MODERN CONTROL DESIGN METHOD II

In this section we will obtain the design using the optimization method. To judge whether the system's performance is optimal, it is customary to use a performance criterion which weights the error e and the control surface deflection δ .

$$V = \int_t^{\infty} (e' Q e + R^2 \delta^2) dt \quad (17)$$

For this performance criterion, the dynamics of the system are given in Sec. (2.2), the state weighting matrix Q is

$$Q = \begin{bmatrix} 1 & 0 & 0 \\ 0 & 0 & 0 \\ 0 & 0 & 0 \end{bmatrix}; \text{ and the control weighting matrix } R \text{ is a scalar.}$$

We want a control gain G which minimizes the performance integral (17). In this case the terminal time is infinite, so the integration (backward in time) will either converge to a constant matrix P or grow without limit. If it converges to a limit, the derivative \dot{P} of (18) tends to zero.

$$-\dot{P} = P A + A' P - P B R^{-1} B' P + Q \quad (18)$$

Hence for an infinite terminal time

$$V_{\infty} = e' \tilde{P} e$$

Where \tilde{P} satisfies the ARE (19) and the optimum gain in the steady state is given by (20).

$$0 = \tilde{P} A + A' \tilde{P} - \tilde{P} B R^{-1} B' \tilde{P} + Q \quad (19)$$

$$G = R^{-1} B' \tilde{P} \quad (20)$$

The ARE (19) is much too complicated to solve analytically, but it can readily be solved by a suitable numerical method. So for finding the control gain matrix G we can plug the matrices Q and R —along with the matrices A and B that define the dynamic process—into a computer program and direct it to find G . If the process is controllable and Q and R are suitable, the computer will not fail to find G .

The numerical values of the elements of the gain matrix G are tabulated for a range of control weighting R in Table 1. Table 1 also shows the closed loop poles and the matrices $B^* E$ and $B^{\#} E$ which constitute the feedforward gain G_0 [2] for the reference input, where

$$B^* = -R^{-1} B' (A_c)^{-1} \tilde{P}$$

$$B^{\#} = (C A_c^{-1} B)^{-1} C A_c^{-1} \quad (21)$$

Table 1 Missile autopilot design results

R	G_e	G_q	G_{δ}	Closed-loop poles	$B^* E$	$B^{\#} E$
E5	-2.090E-3	-.499	5.823	-360.0, -46.0 ± j6.5	1.0755E-3	1.0786E-3
5E5	-.877E-3	-.236	2.561	-176.4, -42.6 ± j13.4	0.5363E-3	0.5433E-3
E6	-.590E-3	-.173	1.796	-139.7, -38.0 ± j16.9	0.5070E-3	0.4169E-3
5E6	-.213E-3	-.086	0.786	-107.5, -25.3 ± j20.4	0.2250E-3	0.2460E-3
E7	-.128E-3	-.063	0.546	-103.7, -20.0 ± j19.9	0.1746E-3	0.2047E-3
5E7	-.278E-4	-.0297	0.223	-100.7, -10.8 ± j17.5	0.0881E-3	0.1457E-3
E8	-.108E-4	-.0206	0.146	-100.3, -8.2 ± j16.8	0.0602E-3	0.1308E-3
E9	.165E-5	-.0046	0.029	-100.03, -3.2 ± j15.8	0.0112E-3	0.1064E-3

From the table, it is seen that as R becomes very large, i.e., the control surface deflection is very heavily weighted, the closed-loop poles approach the open-loop poles. But as the weighting on the control surface is reduced (R is decreased), the complex poles move to the negative open-loop zero on the real axis.

We also note that, the gains B^*E and $B^\#E$ are not equal, although they converge as the control weighting tends to zero, but the discrepancy between the feedforward gains is largest when the control weighting is largest.

Since the missile is stable, the feedback gains can be reduced to zero, which is what happens when the control weighting becomes infinite. But this also reduces the feedforward gain to zero and there is no connection between the reference input (the commanded acceleration) and missile: The achieved acceleration tends to zero leaving a steady state error equal to the commanded acceleration. But it is possible to track the input acceleration perfectly, even without feedback, by use of a feedforward gain given by $G_0 = (CA^{-1}B)CA^{-1}E$ where A is the open-loop dynamics matrix. The numerical value of $G_0 = 0.1064 \times 10^{-3}$ is the feedforward gain that achieves this condition.

5 A COMPARISON OF MODERN AND CLASSICAL DESIGN METHODS.

For comparison between two methods, we select the gain matrix G corresponding to a control weighting of $R = 10^7$ which places the closed-loop poles at $s = -20 \pm j19.9$ which is very close to the values chosen in the pole-placement design. For this value of gain we find that

$$G_0(s) = G(sI - A)^{-1}B = \frac{N(s)}{D(s)} = \frac{40.35s^2 + 4363s + 57628}{(s + 100)(s^2 + 3.33s + 248)}$$

We note that :-

- * The apparent zeros of the loop transmission are both in the left half of the s -plane whereas the pole-placement design had one zero in the right half of the s -plane. This means that the root-locus does not cross into the right half-plane for any value of K .
- * Thus the optimum control design method has an infinite gain margin, and the actual root locus has the appearance shown in Figure (8), but for pole-placement is shown in Figure (6).
- * The dominant poles in both cases are very nearly in the same location ($s \approx -20 \pm j20$) so the transient responses of both systems would be just about the same.
- * Yet the pole-placement design has a finite gain margin while the LQ design of this example has an infinite gain margin.
- * On the other hand, the design method II requires feedback of the actuator state δ . The design method I intentionally eliminated this feedback path.
- * The Bode plots for $G_0(s) = G(sI - A)^{-1}B$ and $G_c(s) = G(sI - A_c)^{-1}B$ for design method II are given in Figure (9), we note that the maximum phase shift of the open-loop transmission is -107° , which provides a phase margin of 73° . While the Bode plots for design method I is shown in Figure (7), which provide a phase margin 50° .
- * Noise sensitivity : larger high-frequency gain of the modern design may result in actuator saturation and control problems in response to guidance noise.

* In most simulated engagements, but not all, the modern autopilot design achieves lower terminal miss distances. It also exhibits faster response to guidance commands than the classical autopilot. This faster response, which may be attributed to the wider bandwidth of the modern design is accompanied by control saturation at 40,000 ft [3].

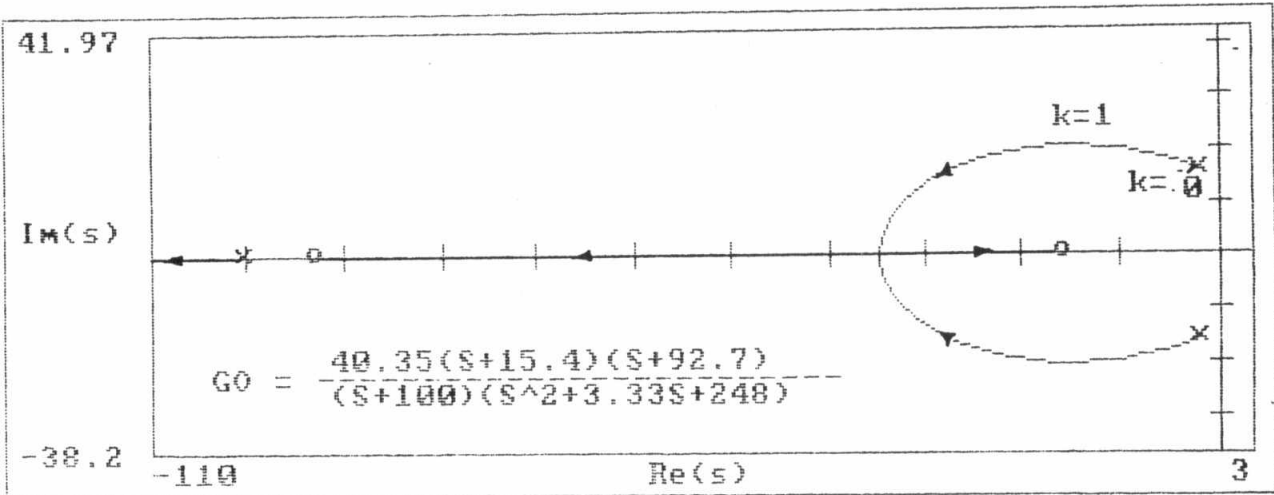


Fig. 8 Root Locus of autopilot design with $R=10^7$.

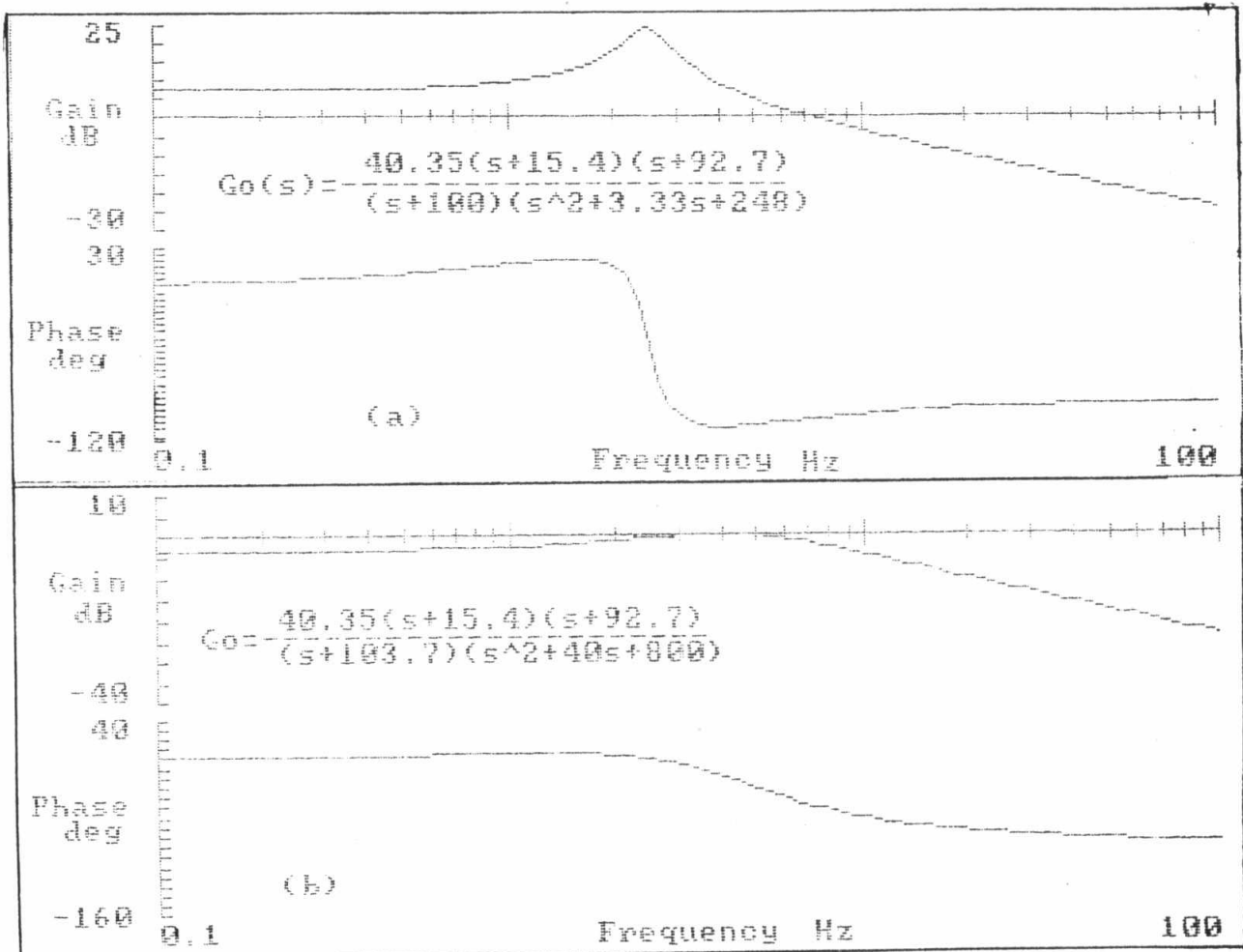


Fig. 9 Bode plots for missile autopilot. (a) Open-loop transmission ; (b) Closed-loop transmission

6 CONCLUSIONS

Modern design techniques have made considerable progress in balancing the requirements of control and robustness to plant uncertainties. Classical design techniques have also progressed by taking advantage of the latest software improvements and modern state-space methods. Modern techniques are well suited for controlling highly coupled airframes, whereas the classical techniques has difficulty finding the proper control law for such systems. The classical technique, however, appears to better account for constraints that are not explicitly modeled. It is recommended that research be continued in both modern and classical techniques and, particularly, in the merging of the two so that design techniques that maintain the best features of both can be developed.

REFERENCES

- [1] Bass, R. W., and Gura, I., "High-Order System Design Via State-Space Considerations," *Proc. Joint Automatic Control Conf.*, Troy, NY, June 1965, pp. 311-318.
- [2] Friedland, B., "Control System Design" Mc Graw Hill co. , New York (1987).
- [3] A. Arrow and D.E. Williams, "Comparison of Classical and Modern Autopilot Design and Analysis Techniques," *Journal of Guidance, Control, and Dynamics*, March-April 1989, Vol.12.
- [4] Blakelock, J.H., "Automatic Control of Aircraft and Missiles" John Wiley & Sons, Inc. , New York (1991).